



Full length article

## A macin identified from *Venerupis philippinarum*: Investigation on antibacterial activities and action mode

Dinglong Yang<sup>a,b</sup>, Yijing Han<sup>a,d</sup>, Lizhu Chen<sup>e</sup>, Ruiwen Cao<sup>a,d</sup>, Qing Wang<sup>a,b</sup>, Zhijun Dong<sup>a,b</sup>, Hui Liu<sup>a,b</sup>, Xiaoli Zhang<sup>a,b</sup>, Qianqian Zhang<sup>a,b</sup>, Jianmin Zhao<sup>a,b,c,\*</sup>

<sup>a</sup> Muping Coastal Environment Research Station, Yantai Institute of Coastal Zone Research, Chinese Academy of Sciences, Yantai, 264003, PR China

<sup>b</sup> Research and Development Center for Efficient Utilization of Coastal Bioresources, Yantai Institute of Coastal Zone Research, Chinese Academy of Sciences, Yantai, 264003, PR China

<sup>c</sup> Center for Ocean Mega-science, Chinese Academy of Sciences, Qingdao, Shandong, 266071, PR China

<sup>d</sup> University of Chinese Academy of Sciences, Beijing, 100049, PR China

<sup>e</sup> Shandong Marine Resource and Environment Research Institute, Yantai, 264006, PR China

### ARTICLE INFO

#### Keywords:

*Venerupis philippinarum*  
Macin  
Molecular characterization  
Antimicrobial activity

### ABSTRACT

In the present study, a macin was cloned and characterized from clam *Venerupis philippinarum* (designed as VpMacin). The full-length cDNA of VpMacin was of 579 bp, encoding a peptide of 87 amino acids with the predicted molecular weight of 9.7 kDa. Analysis of the conserved domain suggested that VpMacin was a new member of the macin family. In non-stimulated clams, VpMacin transcripts exhibited different tissue expression pattern, and highly expressed in the tissues of gills and hepatopancreas. Generally, the temporal expression of VpMacin transcripts was significantly induced in hemocytes of clams post *Vibrio anguillarum* challenge. Moreover, the recombinant VpMacin protein (rVpMacin) showed obvious antimicrobial activities against Gram-positive and Gram-negative bacteria. After incubated with 40 μM rVpMacin, all detected *Escherichia coli* could be killed within 60 min. Membrane integrity analysis revealed that rVpMacin could increase the membrane permeability of bacteria and then resulted in cell death. Overall, our results suggested that VpMacin had an important function in host defense against invasive pathogens.

### 1. Introduction

Antimicrobial peptides (AMPs) are small molecular weight proteins with broad spectrum of antimicrobial activities against bacteria, viruses, and fungi [1]. In eukaryotes, AMPs can be usually classified into three groups: (1) linear alpha-helical peptides without cysteine, such as insect cecropins and magainins; (2) linear peptides with an extended structure constructed by high proportion of one or more amino acids such as proline or histidine; (3) peptides with a looped structure formed by disulfide bonds, such as defensins and protegrin [2]. They can specially function on negatively charged bacterial membranes, subsequently causing membrane disruption or altering metabolic processes by pore formation or by induction of micellization in a detergent-like manner [3,4]. In addition, other functions of AMPs were also proved, such as their anti-tumoural, anti-inflammatory activities, wound-healing and angiogenesis, providing chemoattraction, and promoting nerve repair [5,6].

AMP-encoding genes have been isolated from prokaryotes and eukaryotes, which show a considerable variation in structure and size [7]. Different animals usually possess a reservoir of structurally diverse antibacterial peptides to combat pathogens [8]. In marine invertebrates, different AMPs and their functions have been reported in the innate immune system [9]. To date, four groups of cationic cysteine-rich AMPs have been isolated from mussels *Mytilus galloprovincialis* and *Mytilus edulis*. They were (i) defensin-like peptides MGD-1 and MGD-2 [8,10,11]; (ii) myticins [8]; (iii) mytilins with eight cysteine residues but different specific cysteine arrays and amino acid sequences [8]; and (iv) mytimycin [12]. In addition to the AMPs described above, another type of antimicrobial peptide named macin was recently isolated and characterized from invertebrates [13]. Macin is a member of a large family of small cysteine-rich cationic AMPs [14]. It was originally found in the leech, and usually expressed in immune-related organs/tissues, such as neurons, large fat cells and intestinal epithelia [6]. In neurons, the synthesis of macins participates in the immune responses and the

\* Corresponding author. Muping Coastal Environment Research Station, Yantai Institute of Coastal Zone Research, Chinese Academy of Sciences, Yantai, 264003, PR China.

E-mail address: [jmzhao@yic.ac.cn](mailto:jmzhao@yic.ac.cn) (J. Zhao).

<https://doi.org/10.1016/j.fsi.2019.07.031>

Received 17 April 2019; Received in revised form 4 July 2019; Accepted 11 July 2019

Available online 11 July 2019

1050-4648/© 2019 Elsevier Ltd. All rights reserved.

regeneration of the central nervous system [6,15]. Sequentially, the antibacterial mechanism and mode of action was investigated in hydra [16]. The initial antibacterial step involved aggregating of bacterial cells, and then accompanied by precipitation. The last but not the least, it performed lipid-peptide interactions by electrostatic and hydrophobic effects [16,17].

*Venerupis philippinarum* is an economic species widely spread over many countries. The recent mass mortality of manila clams has been mainly attributed to pathogen invasion and environmental deterioration [18]. Therefore, it is urgently necessary to characterize immune-related molecules for disease control and the healthy management of clam aquaculture. To date, only a few macins have been reported in mollusks, such as *Hyriopsis cumingii* [19] and *Mytilus galloprovincialis* [20]. However, the knowledge on their functions and antibacterial mechanism have not been well investigated in marine bivalves. In the present study, a macin was identified from *V. philippinarum*, and the spatiotemporal expression profiles, bactericidal activities as well as antibacterial action were also investigated to better understand the immune responses of clams against pathogens invasion.

## 2. Materials and methods

### 2.1. Clams and bacterial challenge

Healthy clams *V. philippinarum* with average shell length of 3.0–4.0 cm, were collected from a local aquaculture farm, and maintained in the aerated seawater at 20–22 °C and 30‰ salinity for a week before further processing. The clams were fed with an algae mixture of *Isochrysis galbana* and *Phaeodactylum tricornutum*, and the seawater was totally renewed every day. The clams were randomly divided into six tanks with 50-L capacity and each treatment contained 150 clams. Three tanks served as the control, while the other three tanks were immersed with high density of *V. anguillarum* at a final concentration of  $1 \times 10^7$  CFU mL<sup>-1</sup>. Six individuals from each treatment were randomly sampled at 6, 12, 24 and 48 h post bacterial challenge. Meanwhile, five tissues, including hemocytes, mantle, gills, hepatopancreas and adductor muscle, were collected from 6 individuals of the control group to investigate the tissue-specific expression of VpMacin transcripts.

### 2.2. RNA extraction and cDNA synthesis

Total RNA was extracted from hemocytes, mantle, gills, hepatopancreas and adductor muscle using TRIzol reagent (Invitrogen, USA). RNA quality was assessed by electrophoresis on 1% agarose gel. Total RNA was treated with RQ1 RNase-Free DNase (Promega, USA) to remove DNA contamination. To synthesize cDNA by reverse transcription, 2 µg total RNA, 200 units M-MLV reverse transcriptase (Promega, USA) and 0.5 µM oligo d<sub>T</sub> primer were reacted for 1 h at 42 °C in 25 µL reaction mixture. Then they were terminated by heating at 95 °C for 5 min according to the manufacturer's instruction.

### 2.3. Gene cloning of VpMacin

A macin EST was identified through large scale EST sequencing of the cDNA library constructed [21]. The nested PCR strategy was applied to generate the full-length cDNA of VpMacin (P1 and P2, Table 1). The procedure was listed as follows: the first cycle included an extended (5 min) denaturation period during which polymerase was added (hot-start PCR); 35 cycles of 94 °C for 50 s, 60 °C for 1 min and 72 °C for 1 min; the last cycle had an extended elongation period of 72 °C for 10 min. Semi-nested PCR was performed with the P2 and d<sub>T</sub> using 1 µL of the first round PCR product with the same conditions of the first PCR. 3' RACE PCR products were gel-purified and sequenced. The full-length cDNA of VpMacin was obtained by overlapping the original EST sequence and the amplified fragments.

**Table 1**

Primers used in the present study.

Primer	Sequence (5'-3')	Sequence information
P1	ATGGTCTCGCTGCTCTGGG	3' RACE primer
P2	AGGTAGCGGTAGTTCGGGAGG	3' RACE primer
P3	TGGTCGTCTGCAAGACAAAT	Real-time PCR
P4	TCCCGAACTACCGCTACCTCAA	Real-time PCR
P5	CGCACTTCTCACGCCATCAT	β-actin primer
P6	GCAGCCGTCTCCATTTCTTGTTTC	β-actin primer
P7	CTTGGATCCTCTATCTGGACTGTTGGAAAACAT	Recombinant primer
P8	CGCAAGCTTTCAAGAAGTTTTGCCGTAACATC	Recombinant primer
d <sub>T</sub>	GGCCACGCTGACTAGTACT <sub>17</sub>	Oligo (d <sub>T</sub> )-adaptor

### 2.4. Bioinformatics analysis

The nucleotide sequence was analyzed using the BLAST algorithm at NCBI web site (<http://www.ncbi.nlm.nih.gov/blast>), and the deduced amino acid sequence was analyzed on <http://www.expasy.org/>. The protein domains were predicted with the simple modular architecture research tool version 4.0 (<http://smart.embl-heidelberg.de/>). Multiple alignments were analyzed on <http://www.ebi.ac.uk/clustalw/> and <http://www.bio-soft.net/sms/index.html>.

### 2.5. VpMacin mRNA expression in different tissues and the response to *V. anguillarum* challenge

The spatial and temporal expression profiles of VpMacin mRNA were assayed in an Applied Biosystem 7500 Real-time PCR System. Gene-specific primers (P3 and P4, Table 1) and β-actin primers (P5 and P6, Table 1) were used to amplify the fragments of VpMacin and internal control, respectively. The cycling protocol was 1 cycle of 94 °C for 5 min; 40 cycles of 94 °C for 50 s, 60 °C for 60 s and 72 °C for 50 s followed by 1 cycle of 72 °C for 10 min. The purity of amplification products was evaluated by dissociation curve analysis. The 2<sup>-ΔΔCT</sup> method was used to analyze the relative expression level of VpMacin transcripts [22,23]. All data were given in terms of relative mRNA expressed as mean ± S.D. (N = 6). Statistical analysis was performed by one-way analysis of variance (one-way ANOVA) followed by a Duncan test using SPSS 16.0 software, and P values less than 0.05 were considered statistically significant.

### 2.6. Recombinant expression of VpMacin

Recombinant VpMacin (designed as rVpMacin) was obtained according to our previous study with some modification [24]. Briefly, the fragment encoding mature peptide of VpMacin was amplified with gene-specific primers P7 and P8 with *Bam*H I and *Hind* III sites at their 5' end, respectively (Table 1). The PCR product was purified and sequenced. After digestion with the restriction enzymes *Bam*H I and *Hind* III, the fragment was then cloned into the expression vector pET-30a (+). The rVpMacin was expressed in *Escherichia coli* BL21 (DE3) LysS. Then the rVpMacin peptide was purified by Ni<sup>2+</sup> chelating sepharose column, and refolded in gradient urea-TBS glycerol buffer [25]. Purified rVpMacin was analyzed by 15% SDS-polyacrylamide gel electrophoresis (SDS-PAGE). The concentration of rVpMacin was measured by BCA Protein Assay Kit (Beyotime, China).

### 2.7. Preparation of antibodies and western blotting analysis

The rVpMacin was immunized into 6 weeks old mice to prepare polyclonal antibody against the recombinant protein. The mice were intraperitoneally injected with 100 µg rVpMacin with complete Freund's adjuvant (Sigma, USA) each, and then inoculated with 100 µg

rVpMacin with incomplete Freund's adjuvant (Sigma, USA) two weeks later. The third and fourth injections were given by tail vein with 50  $\mu\text{g}$  rVpMacin at a one-week interval. Seven days after the last injection, the mice were sacrificed to collect immunized serum [26].

For western blotting analysis, the rVpMacin protein was separated using 15% SDS-PAGE. The samples containing rVpMacin were transferred onto nitrocellulose membrane electrophoretically at 200 mA for 45 min after SDS-PAGE. The blotted membrane was blocked with 3% BSA in PBS-T (PBS containing 0.05% Tween-20) at 37 °C for 1 h, and incubated with 1:1000 diluted polyclonal antibody against rVpMacin for 1 h at 37 °C. After washed with PBS-T for three times, goat-anti-mouse Ig-alkaline phosphatase conjugate (Southern Biotech, USA) as second antibody was incubated with the membrane at 37 °C for 1 h. After three washes in PBS-T, positive bands were stained with NBT/BCIP substrate solution for 5 min. As negative control, pre-immunized serum was used instead of immunized serum.

## 2.8. Antimicrobial activity of rVpMacin

The minimal inhibitory concentration (MIC) assay was carried out using six Gram-negative bacteria (*V. anguillarum*, *Vibrio alginolyticus*, *Vibrio harveyi*, *Vibrio splendidus*, *Enterobacter cloacae*, *Pfiodeus mirabidis* and *E. coli*) and one Gram-positive bacteria (*Staphylococcus aureus* and *Micrococcus luteus*) [27]. Briefly, the bacteria were cultured and collected to reach the OD<sub>600</sub> value at 1.0. Then they were diluted 1000-fold in broth. A two-fold serial dilution of rVpMacin was prepared with Tris-HCl buffer (pH 8.0) in sterile 96-well microtiter plates with each column filled with 100  $\mu\text{L}$  of sterilized broth. After that, 5.0  $\mu\text{L}$  of the bacteria suspension were added to the gradient diluted rVpMacin and incubated at their optimum conditions. After 24 h of cultivation, the plate was scanned at 600 nm and the absorbance recorded by a microplate reader (Tecan Infinite M200, Switzerland). The assay was done in triplicate. The MIC value was recorded as the range between the highest concentration of the protein where bacterial growth was observed and the lowest concentration that caused 100% inhibition of bacterial growth.

## 2.9. Time-killing kinetics of rVpMacin

*E. coli* cells were cultured in LB broth to exponential phase for the time-killing assay. After harvested by centrifugation, washed three times with PBS buffer (pH 7.4) and re-suspended in PBS buffer,  $2 \times 10^7$  cells were incubated at 37 °C with 1  $\times$  MIC, 10  $\times$  MIC rVpMacin or PBS (control). The mixture was incubated at 37 °C and withdrew at 0, 10, 30, 60, 160, 360, 600 min after incubation. The number of surviving bacteria, expressed as CFU (colony-forming units), were counted and the time-killing curves were plotted with time against the logarithm of the viable count. Triple independent experiments were performed for time-killing kinetics.

## 2.10. Biofilm formation

Attached biofilm formation was assayed in 96-well polystyrene plates (Corning Costar, USA) with crystal violet staining [28]. Briefly, *E. coli* MG1655 was incubated with rVpMacin at concentrations of 0.1  $\times$  and 1  $\times$  MIC for 8 h. To remove growth effects, we normalized biofilm formation by dividing the total biofilm by the maximal bacterial growth as measured by turbidity at 620 nm. The supernatant was poured out, and the plates were washed three times with room temperature water. After the plates were dried, 300  $\mu\text{L}$  0.1% crystal violet (completely dissolved in water solution) was added in each well for 20 min at room temperature. Then the staining solution was poured out, and the plates were washed three times. 300  $\mu\text{L}$  95% ethanol was added to each well and soaked for 5 min. The total biofilm was measured by turbidity at 540 nm. Ten replicate wells were repeated from two cultures independently.

## 2.11. PAMPs binding assay of rVpMacin

ELISA was performed to examine the PAMPs binding ability of rVpMacin according to previous report [29]. The 96-well microtiter plate was coated with different PAMPs (20  $\mu\text{g}$ /well, in 50 mM carbonate-bicarbonate buffer) at 4 °C overnight, blocked with 3% BSA in PBS at 37 °C for 1 h, and then washed with PBST for three times. Several concentrations of rVpMacin were added and incubated at 18 °C for another 3 h. The wells were then incubated with rVpMacin antibody (1:1000) and goat-anti-mouse Ig-alkaline phosphatase conjugate (1:5000) (Southern Biotech, USA). Finally, pNPP substrate solution was added and incubated at room temperature in dark. The absorbance was measured at 405 nm. The wells with 100  $\mu\text{L}$  of carbonate-bicarbonate buffer were used as blank. As negative control, pre-immunized serum was used instead of immunized serum. Each experiment was performed in triplicate.

## 2.12. Alternations in surface morphology of bacterial cells

*V. splendidus* and *V. anguillarum* cells were cultured in the 2216E culture medium and treated with 1  $\times$  MIC rVpMacin for 60 min at room temperature and immobilized on cover glass slides, respectively. Slide-immobilized cells were fixed with 2.5% (w/v) glutaraldehyde in 0.1 M sodium phosphate buffer for 30 min and dehydrated with a graded ethanol series. After critical-point drying and gold coating, the samples were visualized by scanning electron microscope (SEM, Hitachi S-4800, Japan).

## 2.13. Membrane permeability assay

The outer membrane permeability was determined using the 1-*N*-phenyl-naphthylamine (NPN) uptake assay [30]. Shortly, *E. coli* cells ( $1 \times 10^7$  CFU mL<sup>-1</sup>) were re-suspended in potassium phosphate buffer (pH 7.4). After the addition of NPN at a final concentration of 10  $\mu\text{M}$ , the background fluorescence was recorded at excitation ( $\lambda = 350$  nm) and emission ( $\lambda = 420$  nm). Then, the sample mixtures were incubated with rVpMacin at final concentrations of 0.1  $\times$  MIC, or 1.0  $\times$  MIC for 1 h and the fluorescence was recorded. Each sample was tested in three repetitions and independent assays were performed twice. The results were expressed as relative NPN uptake factors (NPN uptake factor calculated for cells with rVpMacin, subtracted with the NPN uptake factor calculated for cells without rVpMacin).

## 2.14. Determination of membrane potential and permeability by electrochemical assay

Supported bilayer lipid membranes (s-BLMs) were prepared using a paint-freeze method described by White [31]. Briefly, A self-assembly of monolayer (SAM) of 1,2-dipalmitoyl-sn-glycero-3-phosphothioethanol (DPPTE) on the bare gold electrode was prepared by immersing the electrode in a DPPTE solution (2 mmol L<sup>-1</sup> in ethanol) for 16 h. The DPPTE could bind to the gold electrode via Au-S bonding between the electrode surface and the thiol group of DPPTE, thereby producing a SAM on the electrode surface. Then, 5  $\mu\text{L}$  1, 2-dipalmitoyl-sn-glycero-3-phosphocholine (DPPC, 20 mg mL<sup>-1</sup>) in decane was dropped onto the SAM modified electrode. The solvent was then frozen out by placing the electrode at -20 °C for at least 20 min. Subsequently, the electrode surface was submersed in an aqueous solution of 0.1 mol/L KCl for 2 h and rinsed with pure water. Thus, an s-BLMs modified gold electrode was prepared.

Electrochemical measurements were performed on a model 660C Electrochemical Analyzer (CHI Instruments, Inc., Austin, TX) with a PBS buffer (5 mL, 100 mmol L<sup>-1</sup>, pH 6.8) working as electrolyte. A three-electrode system was used for the measurements, in which the modified gold electrode, an Ag/AgCl electrode and a platinum electrode were adopted as the working, reference and counter electrodes,



**Fig. 1.** Multiple alignments of VpMacin with macins from other animals, including *Sinanodonta woodiana* (AIA62156); *Hyriopsis cumingii* (AEC50045); *Aplysia californica* (NP\_001191629); *Stylophora pistillata* (XP\_022810619); *Mytilus galloprovincialis* (CCC15017); *Scapharca broughtonii* (AFQ02694); *Haliotis discus hannai* (AVW85485). Identical residues were marked in dark, and similar amino acids were shaded in gray. Six conserved cysteine residues were labeled by rhombus (▼).

respectively. rVpMacin was added to the electrolyte directly by a microinjector and allowed to interact with s-BLMs for 5 min. The reader of electrochemical measurements is referred to the figure captions for cyclic voltammetry (CV) and electrochemical impedance spectroscopy (EIS) testing parameters.

### 3. Results

#### 3.1. cDNA cloning and sequence analysis of VpMacin

The full-length cDNA of VpMacin was deposited in the GenBank database under the accession no. **KX454482**. The full-length cDNA of VpMacin was of 579 bp, containing a 5' untranslated region (UTR) of 56 bp, and a 3' UTR of 259 bp with a poly (A) tail. The open reading frame (ORF) was 264 bp encoding a peptide of 87 amino acids with the predicted molecular weight of 9.7 kDa. Blast analysis revealed that VpMacin showed high sequence similarities with other known Macins. For example, 58% similarity was observed between VpMacin and macin from *Aplysia californica* (NP\_001191629) (Fig. 1).

#### 3.2. Tissue distribution and temporal expression of VpMacin transcripts after *V. anguillarum* challenge

The distribution of VpMacin mRNA in various tissues of uninfected clams was analyzed by qRT-PCR. VpMacin transcripts were predominantly expressed in gills and hepatopancreas, moderately in hemocytes, and marginally expressed in mantle and muscle (Fig. 2). The temporal expression of VpMacin transcripts in hemocytes of clams post bacterial challenge was shown in Fig. 3. During the first 6 h after pathogen challenge, the expression level of VpMacin mRNA was increased up to 2.26-fold of the control group ( $P < 0.05$ ). After that, the expression level kept increasing and the highest expression level was detected at 12 h post-infection, which was 4.45-fold higher than the control group ( $P < 0.01$ ). As time progressed, the expression of VpMacin transcripts recovered to the original level at 48 h.

#### 3.3. Recombinant expression of VpMacin

The purified protein of rVpMacin was analyzed on 15% SDS-PAGE with an apparent 10 kDa band (Fig. 4, lane 3), which was in accordance with the predicted molecular weight. Western blotting assay was

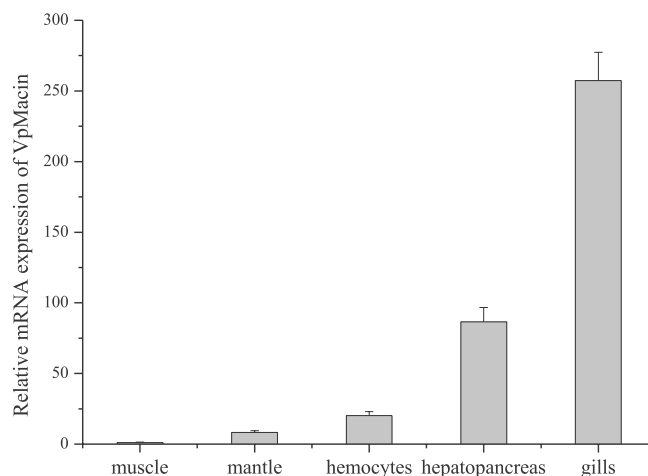


**Fig. 2.** Tissue distribution of VpMacin mRNA detected by qRT-PCR. Transcript level in mantle, gills, hemocytes, and hepatopancreas was normalized to that of muscle. Vertical bars represented the mean  $\pm$  S.D. (N = 6).

performed to identify the specificity of the antibody against clam VpMacin. A clear reaction band representing rVpMacin was immunostained in western blotting, indicating that the antibody could specifically recognize rVpMacin (Fig. 4, lane 4). No reaction band was visible in the negative control (data not shown).

#### 3.4. Antimicrobial activity of rVpMacin

The antimicrobial activity of rVpMacin was investigated against several Gram-positive and Gram-negative bacteria. As revealed in Table 2, rVpMacin displayed obvious antimicrobial activities against Gram-negative bacteria, especially for *V. parahemolyticus*. However, it showed less effective antibacterial activities against *S. aureus* (Table 2).

A time-killing experiment was performed by using *E. coli* as substrate to investigate the bacteriostatic or bactericidal effects of rVpMacin. When *E. coli* was incubated with rVpMacin at a concentration of 10  $\times$  MIC, all bacteria were killed within 60 min (Fig. 5). Meanwhile, the incubation of rVpMacin resulted in less biofilm dispersal of *E. coli* MG1655 on polystyrene surfaces, suggesting that

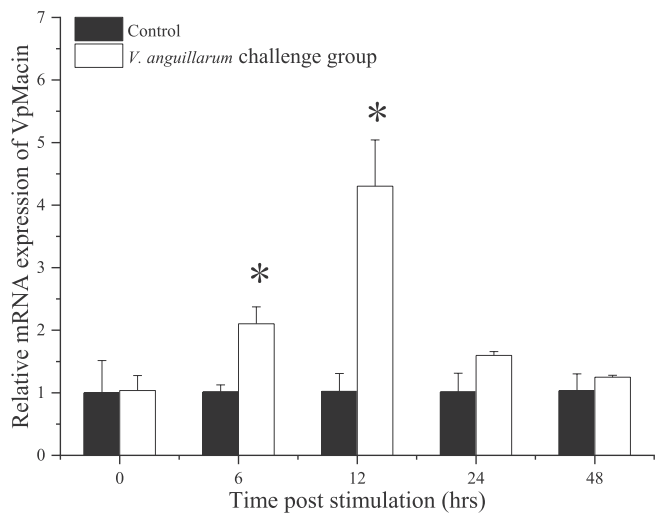


**Fig. 3.** Temporal expression of VpMacin mRNA in hemocytes of clams post *V. anguillarum* challenge. The values were shown as mean ± S.D. (N = 6) (\*:  $P < 0.05$ , \*\*:  $P < 0.01$ ).

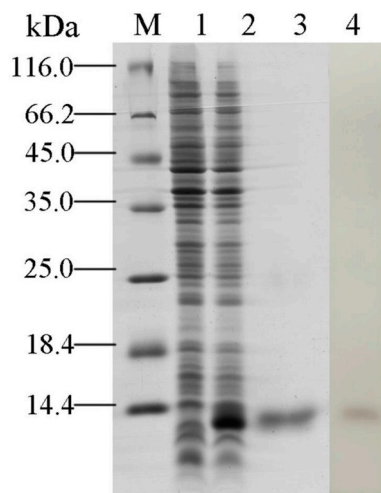


**Fig. 4.** SDS-PAGE and western blotting analysis of rVpMacin. M: protein marker; lane 1: negative control for rVpMacin (without induction); lane 2: induced rVpMacin; lane 3: purified rVpMacin; lane 4: western blotting analysis of rVpMacin.

**Table 2**

Antimicrobial activities of rVpMacin determined by liquid growth inhibition assay.

Microorganisms	MIC value <sup>a</sup> (μM)
Gram-positive bacteria	
Staphylococcus aureus	8.0–16.0
Micrococcus luteus	4.0–8.0
Gram-negative bacteria	
Vibrio anguillarum	2.0–4.0
Vibrio alginolyticus	1.0–2.0
Vibrio parahaemolyticus	0.5–1.0
Vibrio harveyi	1.0–2.0
Vibrio splendidus	1.0–2.0
Enterobacter cloacae	4.0–8.0
Escherichia coli	4.0–8.0
Pfiodeus mirabidis	2.0–4.0

<sup>a</sup>MIC values were expressed as the range between the highest concentration of the protein where bacterial growth was observed and the lowest concentration that caused 100% inhibition of bacterial growth (μM).

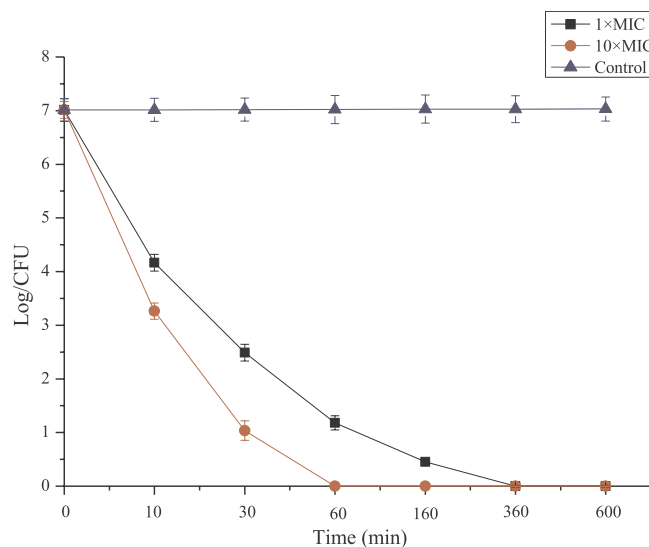


**Fig. 5.** Bacterial killing kinetics of rVpMacin at 1.0× and 10.0× MIC against *E. coli*. The absorbance was recorded at OD<sub>450</sub>. Each group had three replicates.

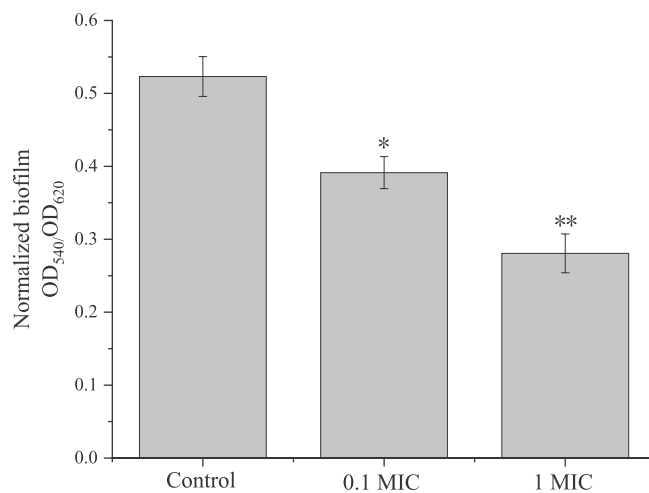


**Fig. 6.** Biofilm formation of *E. coli* MG1655 treated with rVpMacin. Normalized biofilm formation (total biofilm/growth) was tested in 96-well polystyrene plates after treated with rVpMacin. Data were the average of 10 replicate wells from two independent cultures. The values were shown as mean ± S.D. (N = 10) (\*:  $P < 0.05$ , \*\*:  $P < 0.01$ ).

rVpMacin could dramatically reduce the biofilm formation in a concentration-dependent manner (Fig. 6).

### 3.5. PAMPs binding assay of rVpMacin

ELISA was performed to detect the binding activity of rVpMacin towards different PAMPs. The results showed that rVpMacin could bind lipopolysaccharides (LPS), peptidoglycan (PGN), and glucan *in vitro* directly in a dose-dependent manner, but could not bind chitin (Fig. 7). In the control group, no binding activity was observed (data not shown).

### 3.6. Alternations in surface morphology of bacterial cells

SEM experiment was performed to investigate the membrane integrity of *V. anguillarum* and *V. splendidus* in the presence or absence of rVpMacin. In the control group, bacteria displayed a smooth surface without apparent cellular debris (Fig. 8A–C). After incubated with rVpMacin, bacterial cells became shrunken, and the cell surface became obviously roughened and disrupted (Fig. 8B–D).

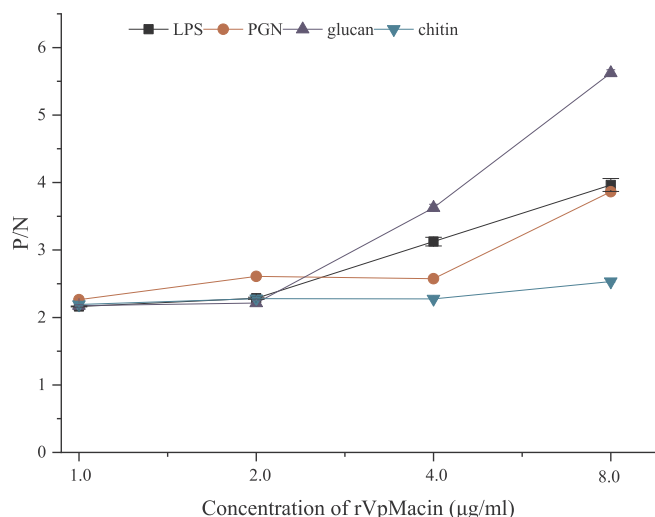


**Fig. 7.** ELISA assay of the interaction between rVpMacin and the PAMPs. Plates were coated with four kinds of PAMPs including LPS, PGN, glucan and chitin, and then incubated with different amounts of rVpMacin. After incubated with rVpMacin antibody and goat-anti-mouse Ig-alkaline phosphatase conjugate, the absorbance was recorded at 405 nm. Samples with P/N > 2.1 were considered positive. Results were representative of the mean of three replicates ± S.D.

**3.7. Disruption of the membrane integrity by rVpMacin**

The NPN assay was used to monitor the outer cell membrane permeabilization. The NPN fluorescence was enhanced to 7.11 when it was incubated with 0.1 × MIC rVpMacin. With the increase of rVpMacin concentration, the NPN fluorescence increased and reached the highest level when incubated with 1 × MIC rVpMacin (Fig. 9). To further investigate the effect of rVpMacin on bacterial membrane, electrochemical assay was employed to observe the effects of mimetic biomembrane in the presence or absence of rVpMacin. As shown in Fig. 10, the incubation of rVpMacin resulted in the increase of charge transfer resistance (Rct), suggesting that rVpMacin could dramatically damage the mimetic biomembrane in a concentration-dependent manner.

**4. Discussion**

Humoral immunity in marine invertebrates is characterized by antimicrobial agents present in the hemolymph, among which AMPs play an important role in the host innate immune responses [32]. Presently, several macins have been identified and characterized in marine invertebrates. However, the knowledge on the functions of macin is still limited in mollusks. In the present study, a new macin was identified

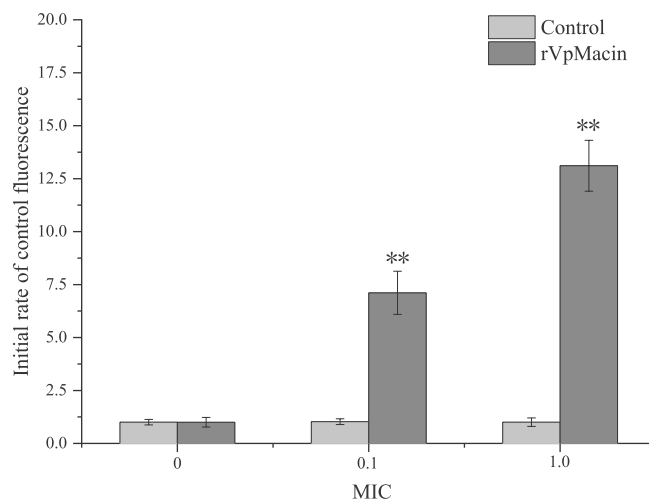


**Fig. 9.** Membrane permeabilization of *E. coli* caused by rVpMacin. Permeabilization of the outer membrane was monitored as an increase in NPN fluorescence intensity in the presence of rVpMacin (0.1 and 1.0 × MIC). Each group had three replicates.

from *V. philippinarum* and its molecular characterization, tissue distribution, antimicrobial activity as well as mode of action were investigated.

The tissue distribution of VpMacin mRNA was dominantly detected in the tissues of gills and hepatopancreas, which were considered as the main tissues involved in the innate immune defense of mollusks. Similarly, the expression of macin transcripts was up-regulated in immune organs of mussel, such as hemocytes and hepatopancreas [12]. The ubiquitous distribution of VpMacin transcripts perhaps contributes to its important roles in immune defense against pathogenic microorganism. Notably, the macin could be expressed in neurons and microglia, and functions as promoters of the regenerative process of axotomized leech central nervous system (CNS) [8]. The specific distribution of macins could be partially explained by their spatial involvement of microbicidal activity or regeneration of the CNS in different organisms.

Moreover, the expression level of VpMacin transcripts was significantly up-regulated in hemocytes post bacterial challenge. The

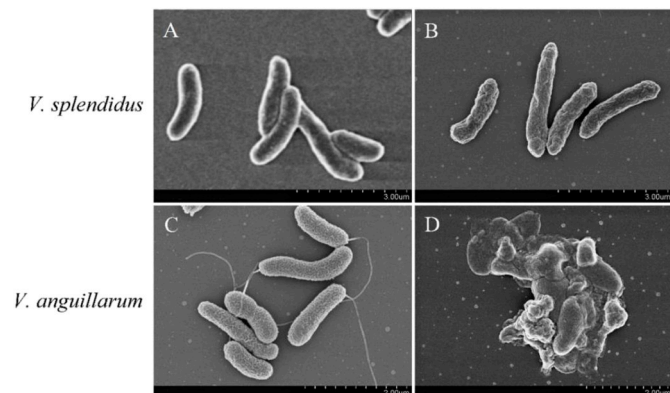


**Fig. 8.** SEM images of bacteria in the absence (A, C) or presence (B, D) of rVpMacin (1.0 × MIC) after exposure for 1 h.

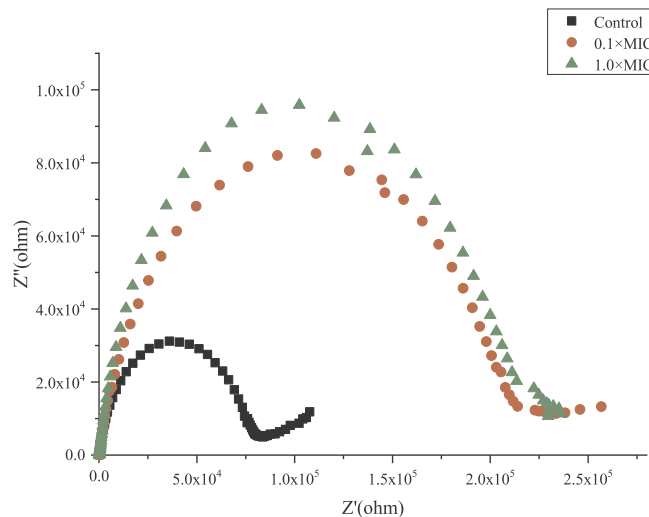


**Fig. 10.** Impedance complex plane plots of s-BLMs coated gold electrode in the presence of rVpMacin. 0.1 × and 1.0 × MIC rVpMacin was added to the electrolyte directly by a micro-injector and allowed to interact with s-BLMs for 5 min, respectively. EIS was carried out over a frequency range of 0.01 Hz–100 kHz at a signal amplitude of 10 mV.

increase of VpMacin in the early stage might be ascribed to considerable recruitment of VpMacin-producing hemocytes into/near the infection site. As reported by Allam et al., circulating hemocytes was increased rapidly in *V. philippinarum* after challenged by *V. anguillarum* and *Vibrio tapetis* [33]. All these results suggested that VpMacin had an important function in host defense against invasive pathogens.

In the present study, the MIC of rVpMacin towards different bacteria ranged from 0.5 to 16.0  $\mu\text{M}$ , and other macins (e.g. theromacin from leeches) showed similar inhibitory activity towards tested microorganisms (MBC: 0.39–100  $\mu\text{g}/\text{mL}$ ) [34]. Notably, the Gram-positive bacterium *Bacillus megaterium* ATCC 14581 was killed by theromacin in a low concentration (MBC: 0.39  $\mu\text{g}/\text{mL}$ ). Taking into consideration of the three-dimensional structure of theromacin, the high antibacterial activity might be induced by the long N-terminal region with two residues (Asp<sup>5</sup> and Asp<sup>23</sup>) [34]. In the present study, almost all *E. coli* were killed within 60 min after being incubated with 10  $\times$  MIC rVpMacin. Parallel to these results, defensin from *V. philippinarum* could eliminate all examined bacteria within a few minutes [20]. These results suggested that VpMacin was perhaps coupled with other antibacterial peptides to eliminate invading bacteria.

The biofilm formation of *E. coli* was significantly depressed by rVpMacin even at low concentrations. Similar study was also supported in other immune-related peptides, such as LL-37 [35], and defensin [36]. For example, human LL-37 could decrease the biofilm formation even at 0.5  $\mu\text{g}/\text{mL}$ , which was far below those required to kill or inhibit bacterial growth. They might reduce the initial attachment of invading bacteria, cause bacteria to wander across the surface instead of forming biofilm, and down-regulate key components expression, especially the essential genes of biofilm development and maintenance [37,38].

Previous studies have suggested that some AMPs exerted their antibacterial activity based on their damage to bacterial membranes or cell walls. In Hydra, a stronger interaction was found between LPS and hydramacin-1, thus may lead to aggregation of invasive bacteria as an initial step of its bactericidal mechanism [9]. Meanwhile, lipid could also be recognized by hydramacin-1. The lipid-hydramacin-1 interaction might be initiated by electrostatic and hydrophobic effects, in particular, by tryptophan and neighboring polar amino acid residues. The high binding constants of hydramacin-1 upon lipid interaction also contributes to their aggregation and antibacterial activities [17,34]. In this work, rVpMacin could bind to LPS, PGN and glucan in a concentration-dependent manner, which perhaps indicated that the affinity to PAMPs was a vital step for immune responses [39]. More notably, some AMPs (e.g. LL-37, neuromacin, magainin and macrolittins) could kill invading bacteria by membrane dysfunction (pore forming) [40]. In basal metazoan hydra, hydramacin-1 could interfere with the polymerization or depolymerization of filaments, thus lead to invaginations or formation of protuberances of the bacterial membrane [16]. In the present study, deleterious effects of rVpMacin on the bacterial membrane of tested bacteria were investigated by monitoring membrane permeability. rVpMacin (0.1  $\times$  and 1.0  $\times$  MIC) induced a similar increase of fluorescence and noticeable changes of membrane permeability. Meanwhile, both *V. splendidus* and *V. anguillarum* were chosen for the morphology test. They were potential pathogens for manila clams, which could induce disturbances in energy metabolism and osmotic regulation, oxidative and immune stresses [41,42]. The results suggested that bacterial membrane was potential target where rVpMacin might function on. Furthermore, in the electrochemical assay, rVpMacin intercalated chiefly into the outer layer, amplifying the steric hindrance effect, thereby resulting in an increased Rct. In turmeric, curcumin could interact with the self-assembled bilayer lipid membranes with two manners. At low concentrations, curcumin tends to insert into the outer monolayer only, while at high concentrations, it may also begin to penetrate the inner monolayer [43]. These above results supported the hypothesis that the bacterial bilayer-lipid membrane was one of the potential targets of VpMacin-induced toxicity.

In conclusion, a macin peptide was characterized from *V.*

*philippinarum*, and the expression profiles, antimicrobial activities and mode of action were investigated. These results would provide helpful evidence for a better understanding of the innate immunity of the manila clam. To further broaden our knowledge on the antibacterial mechanism of VpMacin, future efforts on the interaction of macin with membranes or cell walls of bacteria were required.

## Acknowledgements

This research was supported by grants from the National Natural Science Foundation of China (No. 41476126 and 41806196), the Key Research Program of the Chinese Academy of Sciences (No. KFJ-STZ-DTP-023), Natural Science Foundation of Shandong Province (ZR2019BD022) and the Youth Innovation Promotion Association of CAS (2016196).

## References

- [1] M. Zasloff, Antimicrobial peptides of multicellular organisms, *Nature* 415 (6870) (2002) 389–395.
- [2] D.A. Devine, R.E.W. Hancock, Cationic peptides: distribution and mechanisms of resistance, *Curr. Pharmaceut. Des.* 8 (9) (2002) 703–714.
- [3] K.A. Brogden, Antimicrobial peptides: pore formers or metabolic inhibitors in bacteria? *Nat. Rev. Microbiol.* 3 (3) (2005) 238–250.
- [4] J.D. Hale, R.E. Hancock, Alternative mechanisms of action of cationic antimicrobial peptides on bacteria, *Expert Rev. Anti Infect.* 5 (6) (2007) 951–959.
- [5] T. Ayabe, T. Ashida, Y. Kohgo, T. Kono, The role of Paneth cells and their antimicrobial peptides in innate host defense, *Trends Microbiol.* 12 (8) (2004) 394–398.
- [6] A.J. Otero-Gonzalez, B.S. Magalhaes, M. Garcia-Villarino, C. Lopez-Abarrategui, D.A. Sousa, S.C. Dias, O.L. Franco, Antimicrobial peptides from marine invertebrates as a new frontier for microbial infection control, *FASEB J.* 24 (5) (2010) 1320–1334.
- [7] R. Bals, J.M. Wilson, Cathelicidins - a family of multifunctional antimicrobial peptides, *Cell. Mol. Life Sci.* 60 (4) (2003) 711–720.
- [8] G. Mitta, F. Vandenbulcke, F. Hubert, M. Salzet, P. Roch, Involvement of mytilins in mussel antimicrobial defense, *J. Biol. Chem.* 275 (17) (2000) 12954–12962.
- [9] J.A. Tincu, S.W. Taylor, Antimicrobial peptides from marine invertebrates, *Antimicrob. Agents Chemother.* 48 (10) (2004) 3645–3654.
- [10] J.K. Seo, J.M. Crawford, K.L. Stone, E.J. Noga, Purification of a novel arthropod defensin from the American oyster, *Crassostrea virginica*, *Biochem. Biophys. Res. Commun.* 338 (4) (2005) 1998–2004.
- [11] Y. Gueguen, A. Herpin, A. Aumelas, J. Garnier, J. Fievet, J.M. Escoubas, P. Bulet, M. Gonzalez, C. Lelong, P. Favrel, E. Bachere, Characterization of a defensin from the oyster *Crassostrea gigas* - recombinant production, folding, solution structure, antimicrobial activities, and gene expression, *J. Biol. Chem.* 281 (1) (2006) 313–323.
- [12] M. Charlet, S. Chernysh, H. Philippe, C. Hetru, J.A. Hoffmann, P. Bulet, Innate immunity - isolation of several cysteine-rich antimicrobial peptides from the blood of a mollusc, *Mytilus edulis*, *J. Biol. Chem.* 271 (36) (1996) 21808–21813.
- [13] A. Tasiemski, F. Vandenbulcke, G. Mitta, J. Lemoine, C. Lefebvre, P.E. Sautiere, M. Salzet, Molecular characterization of two novel antibacterial peptides inducible upon bacterial challenge in an annelid, the leech *Theromyzon tessulatam*, *J. Biol. Chem.* 279 (30) (2004) 30973–30982.
- [14] C.W. Hung, S. Jung, J. Grotzinger, C. Gelhaus, M. Leippe, A. Tholey, Determination of disulfide linkages in antimicrobial peptides of the macin family by combination of top-down and bottom-up proteomics, *J. Proteom.* 103 (2014) 216–226.
- [15] D. Schikorski, V. Cuvillier-Hot, M. Leippe, C. Boidin-Wichlacz, C. Slomianny, E. Macagno, M. Salzet, A. Tasiemski, Microbial challenge promotes the regenerative process of the injured central nervous system of the medicinal leech by inducing the synthesis of antimicrobial peptides in neurons and microglia, *J. Immunol.* 181 (2) (2008) 1083–1095.
- [16] S. Jung, A.J. Dingley, R. Augustin, F. Anton-Erxleben, M. Stanisak, C. Gelhaus, T. Gutschmann, M.U. Hammer, R. Podschun, A.M.J.J. Bonvin, M. Leippe, T.C.G. Bosch, J. Grotzinger, Hydramacin-1, structure and antibacterial activity of a protein from the basal metazoan hydra, *J. Biol. Chem.* 284 (3) (2009) 1896–1905.
- [17] M. Michalek, B. Vincent, R. Podschun, J. Grotzinger, B. Bechinger, S. Jung, Hydramacin-1 in action: scrutinizing the barnacle model, *Antimicrob. Agents Chemother.* 57 (7) (2013) 2955–2966.
- [18] B. Allam, C. Paillard, S.E. Ford, Pathogenicity of *Vibrio tapetis*, the etiological agent of brown ring disease in clams, *Dis. Aquat. Org.* 48 (3) (2002) 221–231.
- [19] Q.Q. Xu, G.L. Wang, H.W. Yuan, Y. Chai, Z.L. Xiao, cDNA sequence and expression analysis of an antimicrobial peptide, theromacin, in the triangle-shell pearl mussel *Hyriopsis cumingii*, *Comp. Biochem. Physiol.* B 157 (1) (2010) 119–126.
- [20] M. Gerdol, G. De Moro, C. Manfrin, P. Venier, A. Pallavicini, Big defensins and mytimacins, new AMP families of the Mediterranean mussel *Mytilus galloprovincialis*, *Dev. Comp. Immunol.* 36 (2) (2012) 390–399.
- [21] J.M. Zhao, C.H. Li, A.Q. Chen, L.Y. Li, X.R. Su, T.W. Li, Molecular characterization of a novel big defensin from clam *Venerupis philippinarum*, *PLoS One* 5 (10) (2010) e13480.
- [22] K.J. Livak, T.D. Schmittgen, Analysis of relative gene expression data using real-

- time quantitative PCR and the 2(T)(-Delta Delta C) method, *Methods* 25 (4) (2001) 402–408.
- [23] Y.Y. Zhang, Q. Wang, Y.L. Ji, Q. Zhang, H.F. Wu, J. Xie, J.M. Zhao, Identification and mRNA expression of two 17 beta-hydroxysteroid dehydrogenase genes in the marine mussel *Mytilus galloprovincialis* following exposure to endocrine disrupting chemicals, *Environ. Toxicol. Pharmacol.* 37 (3) (2014) 1243–1255.
- [24] D.L. Yang, Q. Wang, R.W. Cao, L.Z. Chen, Y.L. Liu, M. Cong, H.F. Wu, F. Li, C.L. Ji, J.M. Zhao, Molecular characterization, expression and antimicrobial activities of two c-type lysozymes from manila clam *Venerupis philippinarum*, *Dev. Comp. Immunol.* 73 (2017) 109–118.
- [25] Q. Wang, C.Y. Wang, C.K. Mu, H.F. Wu, L.B. Zhang, J.M. Zhao, A novel c-type lysozyme from *Mytilus galloprovincialis*: insight into innate immunity and molecular evolution of invertebrate c-type lysozymes, *PLoS One* 8 (6) (2013) e67469.
- [26] P.K. Smith, R.I. Krohn, G.T. Hermanson, A.K. Mallia, F.H. Gartner, M.D. Provenzano, E.K. Fujimoto, N.M. Goeke, B.J. Olson, D.C. Klenk, Measurement of protein using bicinchoninic acid, *Anal. Biochem.* 150 (1) (1985) 76–85.
- [27] L.B. Zhang, D.L. Yang, Q. Wang, Z.Y. Yuan, H.F. Wu, D. Pei, M. Cong, F. Li, C.L. Ji, J.M. Zhao, A defensin from clam *Venerupis philippinarum*: molecular characterization, localization, antibacterial activity, and mechanism of action, *Dev. Comp. Immunol.* 51 (1) (2015) 29–38.
- [28] L.A. Pratt, R. Kolter, Genetic analysis of *Escherichia coli* biofilm formation: roles of flagella, motility, chemotaxis and type I pili, *Mol. Microbiol.* 30 (2) (1998) 285–293.
- [29] Y.H. Yu, Y.C. Yu, H.Q. Huang, K.X. Feng, M.M. Pan, S.C. Yuan, S.F. Huang, T. Wu, L. Guo, M.L. Dong, S.W. Chen, A.L. Xu, A short-form C-type lectin from amphioxus acts as a direct microbial killing protein via interaction with peptidoglycan and glucan, *J. Immunol.* 179 (12) (2007) 8425–8434.
- [30] D. Nievagomez, J. Konisky, R.B. Gennis, Membrane Changes in *Escherichia coli* induced by colicin ia and agents known to disrupt energy transduction, *Biochemistry-U S* 15 (13) (1976) 2747–2753.
- [31] S.H. White, Temperature-dependent structural-changes in planar bilayer membranes - solvent freeze-out, *Biochim. Biophys. Acta* 356 (1) (1974) 8–16.
- [32] R.E.W. Hancock, G. Diamond, The role of cationic antimicrobial peptides in innate host defences, *Trends Microbiol.* 8 (9) (2000) 402–410.
- [33] B. Allam, S.E. Ford, Effects of the pathogenic *Vibrio tapetis* on defence factors of susceptible and non-susceptible bivalve species: I. Haemocyte changes following in vitro challenge, *Fish Shellfish Immunol.* 20 (3) (2006) 374–383.
- [34] S. Jung, F.D. Sonnichsen, C.W. Hung, A. Tholey, C. Boidin-Wichlacz, W. Haeusgen, C. Gelhaus, C. Desel, R. Podschun, V. Waetzig, A. Tasiemski, M. Leippe, J. Grotzinger, Macin family of antimicrobial proteins combines antimicrobial and nerve repair activities, *J. Biol. Chem.* 287 (17) (2012) 14246–14258.
- [35] J. Overhage, A. Campisano, S. Haussler, B. Rehm, R. Hancock, Human host defense peptide LL-37 prevents bacterial biofilm formation, *Int. J. Med. Microbiol.* 299 (2009) 74–74.
- [36] D.L. Yang, Q.Q. Zhang, Q. Wang, L.Z. Chen, Y.L. Liu, M. Cong, H.F. Wu, F. Li, C.L. Ji, J.M. Zhao, A defensin-like antimicrobial peptide from the manila clam *Ruditapes philippinarum*: investigation of the antibacterial activities and mode of action, *Fish Shellfish Immunol.* 80 (2018) 274–280.
- [37] P.K. Singh, M.R. Parsek, E.P. Greenberg, M.J. Welsh, A component of innate immunity prevents bacterial biofilm development, *Nature* 417 (6888) (2002) 552–555.
- [38] C. Picioreanu, J.U. Kreft, J.A.J. Haagensen, T. Tolker-Nielsen, S. Molin, Microbial motility involvement in biofilm structure formation - a 3D modelling study, *Water Sci. Technol.* 55 (8–9) (2007) 337–343.
- [39] M.R. Yeaman, N.Y. Yount, Mechanisms of antimicrobial peptide action and resistance, *Pharmacol. Rev.* 55 (1) (2003) 27–55.
- [40] K. Sivieri, J. Bassan, G. Peixoto, R. Monti, Gut microbiota and antimicrobial peptides, *Curr. Opin. Food Sci.* 13 (2017) 56–62.
- [41] D. Castro, M.J. Pujalte, L. Lopez-Cortes, E. Garay, J.J. Borrego, *Vibrios* isolated from the cultured manila clam (*Ruditapes philippinarum*): numerical taxonomy and antibacterial activities, *J. Appl. Microbiol.* 93 (3) (2002) 438–447.
- [42] X.L. Liu, C.L. Ji, J.M. Zhao, H.F. Wu, Differential metabolic responses of clam *Ruditapes philippinarum* to *Vibrio anguillarum* and *Vibrio splendidus* challenges, *Fish Shellfish Immunol.* 35 (6) (2013) 2001–2007.
- [43] G.F. Chen, Y.Y. Chen, N.N. Yang, X.J. Zhu, L.Z. Sun, G.X. Li, Interaction between curcumin and mimetic biomembrane, *Sci. China Life Sci.* 55 (6) (2012) 527–532.